Structure of 60° dislocations at the GaAs/Si interface

A. Vilà, A. Cornet, and J. R. Morante
LCMM, Dept. Física Aplicada i Electrònica, Universitat de Barcelona, Diagonal 645-647, 08028 Barcelona, Spain

P. Ruterana
LERMAT, Université de Caen, 6 Bld Maréchal Juin, 14050 Caen, France

M. Loubradou and R. Bonnet
Institut National Polytéchnique, LTPCM, ENSEEG, Domaine Universitaire, BP 44, 38401 Saint Martin D'Hères, France

(Received 3 January 1995; accepted for publication 12 October 1995)

High-resolution electron microscopy technique has been applied to a detailed study of the 60° dislocations at the atomic layer molecular-beam-epitaxial GaAs/Si interface. Their deformation fields strongly interact with neighbor dislocations inducing irregular spacing between the cores and possible dissociations. Biatomic silicon steps were observed at the interface, but never inside 60° dislocation cores. Computer image simulation and elasticity calculations of the atomic displacement field have been used in order to determine the structure of the 60° dislocation; however, due to the Eshelby effect and to interaction with some neighbor dislocations, in many cases no theoretical model could explain some observations. © *1996 American Institute of Physics.* [S0021-8979(96)06302-2]

I. INTRODUCTION

For a number of years, there has been high activity in the molecular-beam-epitaxy (MBE) growth of GaAs on Si substrates mainly for the high-quality, low-cost, high thermal conductivity, and mechanical strength of the Si substrates, as well as for the direct visible gap and high mobility of GaAs. Eventually, the aim is to combine the optoelectronical properties of GaAs and the well developed technology on silicon, i.e., monolithic integration of GaAs and Si technology.

The growth of high-quality GaAs on Si has for a long time confronted three major problems: the 4% lattice mismatch between the two materials, the 60% difference in the thermal-expansion coefficient, and the formation of inversion domains in the polar epitaxial layer. The nature of the defects that nucleate at the interface plays a crucial role in the GaAs layer structure and final properties. These defects can be Lomer and 60° dislocations, as well as stacking faults and inversion boundaries and, as growth occurs in a three-dimensional mode, grain boundaries can also form. Among these defects, the 60° dislocation has a very peculiar role in the degradation of the properties of the GaAs layer. This type of dislocation has its Burgers vector and dislocation line along {111} crystallographic planes of easy slip in GaAs, so they can easily move up through the layer and thread toward the surface.[1] The threading lines can cause enhanced impurity diffusion, partial short circuits for *p-n* junctions, and the degradation of optical and electrical properties of the epilayers.

At the point view of structure, a large number of results exists on the study of the 60° dislocation in bulk materials. Most of them are based on the model proposed by Shockley in 1953[2] for diamond materials, whose detailed structure was sketched and used to describe the core and jogs of the other dislocation types possible in diamond lattice by Hornstra.[3] However, a quite general conclusion can be that under stress it always decomposes into its 90° and 30° partials giving rise to a stacking fault in between. The two partials can be more or less widely spaced.[4–6] Especially in GaAs the 30° partial has been recently studied using high-resolution transmission electron microscopy (HREM).[7] It was also shown that the 60° dislocation can participate in the formation of antiphase boundaries and in their subsequent deviation from {110} planes toward {11*n*}-type planes.[8] In the conventional MBE, the 60° dislocation density can be as large as 50% of that of Lomer dislocation at the GaAs/Si interface; one way of decreasing it was by making the GaAs growth on misoriented (001) Si substrates,[1] in which case the number of Lomer dislocations was ~30 times higher than that of the 60° ones.

The 60° dislocation at an interface has been at times associated to the presence of steps due to the (002) half-plane terminating in its core. Although no HREM work using image simulations for models has been published, there has been put forward essentially two 60° dislocation structures for GaAs/Si. Results of Otsuka *et al.*[1] suggest the generation of 60° dislocation on terraces while Lomer ones are favored by steps, and those of Tsai and Lee[9] indicate that there are steps located inside the 60° cores. The two configurations were similar to the model described by Shockley.[2]

More recently, mechanisms depending on the growth mode of GaAs on Si have been proposed for the generation of 60° dislocations at their interface. As for the majority of the mismatched materials, the growth of GaAs on Si takes place in a more or less three-dimensional way. Thus, it has been argued that Lomer dislocations are nucleated inside islands and 60° ones preferentially nucleate when individual islands join to form a continuous layer.[10] Accordingly, it has been rather usual to try to devise a growth method which would lead to low density of defects in the GaAs layer and the best results seem to have been obtained when a pseudotwo-dimensional growth mode could be approached.[11] This is quite in agreement with our previous results which

 0021-8979/96/79(2)/676/6/$6.00

indicate that the atomic layer molecular-beam-epitaxy (ALMBE) growth is more two dimensional than the conventional MBE.[12] In the ALMBE GaAs on nonmisoriented (001) Si wafer, the number of 60° dislocations is only 14% of the total number of dislocations[13] instead 30% in the conventional MBE.[1]

In this work we have investigated the atomic structure of the core of 60° dislocations located at the GaAs/Si interface running along ⟨110⟩ directions, and at a few nm inside the GaAs layer. The basic tools used were HREM, anisotropic elasticity calculations, and image simulation of model structures. These dislocations were found to interact with the nearby ones and to lead to their decomposition.

II. EXPERIMENT

The GaAs layers were grown by using the ALMBE growth technique developed by Briones, González, and Ruiz,[14] which consists on the combination of a continuous element III flux with an alternating periodic element V flux matched to the speed of 1 monolayer deposition. The substrate was exact (001) Si. The growth was started by opening the Ga cell and, after 1 monolayer deposition, GaAs was grown by ALMBE. The substrate temperature was kept at 300 °C with a thermal annealing up to 580 °C after the first 200 nm and after the complete growth.

For conventional transmission electron microscopy (TEM) examination, [110] and [1$\bar{1}$0] specimens were cut, polished, and ion milled with Ar^+ according to the standard methods, until reaching the thickness of ~10 nm necessary for high-resolution imaging.

Observations were carried out in a Philips EM-430ST operated at 300 kV. Its spherical aberration coefficient C_s was 1.1 mm and the beam semiconvergence 0.8 mrad. Energy instabilities lead to a focus spread of 10 nm. With these characteristics, the Scherzer focus is reached for $\Delta f = 57.0$ nm, where the point resolution is ~0.2 nm. At defocusing distances up to this, good imaging can be obtained for both GaAs and Si perfect crystals. As the correspondence between the intensity in the image and the projected potential is nonlinear and noninvertible, the only way to determine the inner core structure consists in a trial-and-error method on image simulations of various model structures. In this work, multislice calculations were made using the electron microscopy Software (EMS) simulation package of Stadelmann.[15] The main parameters for contrast interpretation in high-resolution images (sample thickness and defocusing distance) were accurately determined by comparing experimental and simulated images using the above microscope parameters.

The models were provided by elasticity calculations using the theoretical formalism developed by Bonnet, Marcon, and Ati.[16] In their misfit formalism, contrarily to the translation dislocations which are supposed to be perfect, a regular array of dislocations with a very small Burgers vector is superimposed to the perfect dislocations at the interface. Thus, the misfit formalism gives a displacement which changes linearly along the interface with a discontinuity at the position of a perfect dislocation core (Fig. 1). The elasticity equations are solved in a two-dimensional framework.

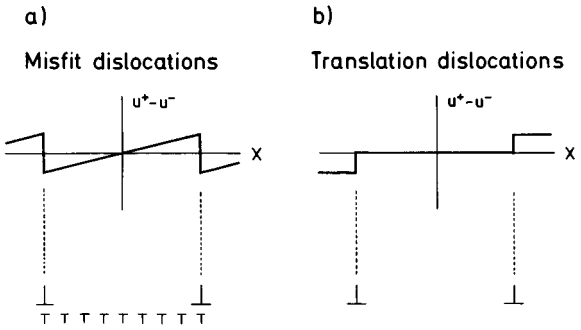

FIG. 1. Displacement vs position along the interface for (a) misfit and (b) translation dislocation formalisms. Note that displacements will coincide at the middle position between two subsequent perfect dislocations.

More details about experiment, calculations, and simulation are given in a previous work.[13]

III. RESULTS AND DISCUSSION

In GaAs/Si interface, the 4% lattice mismatch is relaxed mainly by dislocations located at the interface, as shown in Fig. 2 where HREM images of the interface viewed along [110] and [1$\bar{1}$0] zone axes are presented in (a) and (b), respectively. A general feature is that individual 60° dislocations (14% of the total number of interfacial defects) are found between two Lomer dislocations. Spacing between the 60° one and its neighbor at each side is quite asymmetric, with a difference of about 3.5 nm. When two 60° dislocations are adjacent, the distance to neighboring Lomers is smaller (about 4.0 nm).

The dislocation of 60° type has a significant edge component in the plane of view and would therefore seem appropriate for high-resolution observation; however, its analysis

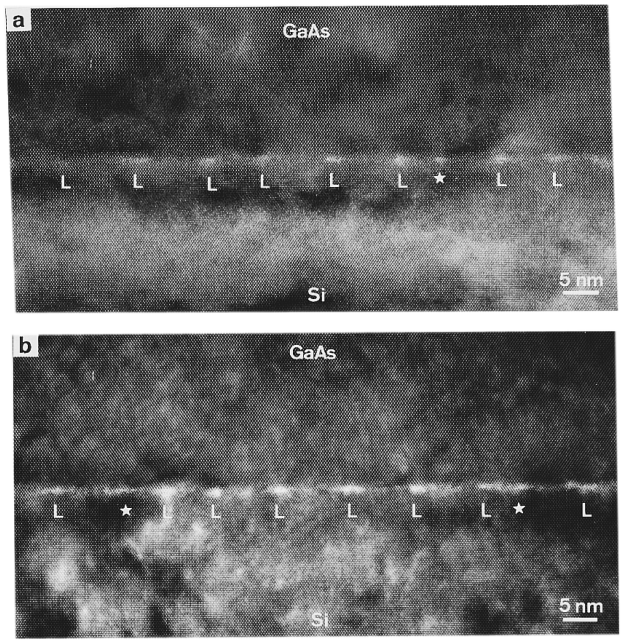

FIG. 2. HREM image of the GaAs/Si interface viewed along [110] in (a) and [1$\bar{1}$0] zone axis in (b). Lomer dislocations are denoted with *L* and 60° ones with *.

at atomic scale is more difficult than for the Lomer dislocation because the screw component can introduce a local crystal rotation complicating the interpretation of the observed image contrast. This distortion affects the area around the core and can extend to neighboring interface defects. Hence, the deformation field strongly interacts with other dislocations, often causing dissociations and extended cores. The dislocation line may have kinks, lying away from the exact $\langle 110 \rangle$ direction; however, this study has been carried out on dislocations which show no evidence of this behavior, as images do not move appreciably in a through focus series.

These are reasons why, among the 60° dislocations observed, only few showed good enough contrast for a detailed analysis in the light of existing models. Two cases could be analyzed in detail and simulated using elastical models: One corresponding to a perfect dislocation located at the interface and the other found inside the GaAs layer but showing very strong interaction with dislocations at the interface. For all other dislocations the contrast and hence the structure changed from one to the next. In the first subsection 60° interfacial dislocations are discussed, and the perfect core and other cases are treated individually. Finally, the compact core located out of, but near the interface, is analyzed in detail and simulated via elasticity models.

What is remarkable in these samples is that the strain field around a 60° dislocation at the interface can interact with the neighboring ones and can lead to their dissociation. This report is only devoted to the 60° dislocation structure and the different types of dissociation for neighboring Lomer dislocations are complex, and will be the subject of a separate report. Moreover, the total spacing between the two neighbors of a 60° dislocation can be related to the direction of the 60° Burgers vector. To put this relation in evidence, let us take as reference the dislocation line along the $[110]$ or $[1\bar{1}0]$ direction. When the distance is larger than that predicted for relaxation (defects not effective enough to completely relax the misfit) the Burgers vector found points to the substrate and has one of these two forms:

$$\mathbf{b} = 1/2[101] \quad \text{or} \quad 1/2[0\bar{1}1].$$

On the contrary, if the total spacing is smaller (defects more effective than necessary to relax) it points to the layer and is

$$\mathbf{b} = 1/2[10\bar{1}] \quad \text{or} \quad 1/2[01\bar{1}].$$

It is not possible to distinguish the two possibilities in each case because the projection of the Burgers vector onto the image plane gives no information about the screw component.

A. The perfect 60° core

The first model for the 60° dislocation core in bulk material is due to Shockley,[2] having one dangling bond per unit cell (Fig. 3). It was obtained by adding an atomic couple to an individual six-atom ring limiting the two terminating (111) and (002) half-planes. One stepped model has also been proposed in the glide set to describe 60° dislocations with similar characteristics but located at silicon surface steps.[9] However, none of the 60° dislocations analyzed in this work was associated to an extra Si (002) half-plane on the substrate surface. In the following, the experimental images are presented in the light of anisotropic elasticity configurations,[17] and they are related to the Shockley model which, as for the Lomer dislocation,[3] was proposed in order to account for the core of 60° dislocations in bulk diamond lattices.

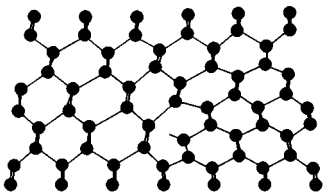

FIG. 3. Schematic configuration of 60° dislocation as described by Shockley.

Figures 4(a) and 4(b) show this type of dislocation image at 34 and 70 nm defocus, respectively. From these images, an attempt to determine the atomic positions inside the dislocation core can be made. For the anisotropic elasticity calculations the input was the ideal period for an array of alternating Lomer and 60° dislocations at the interface, and

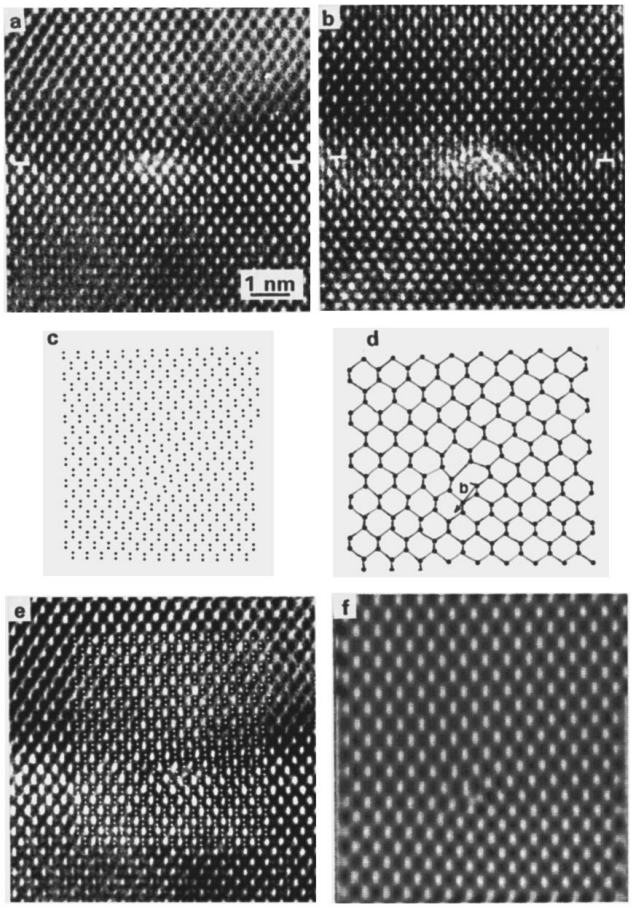

FIG. 4. Experimental image of an ideal 60° dislocation core at the GaAs/Si interface. Δf is ~34 nm in (a) and ~70 nm in (b). The model predicted by elastical calculation and the bonding in the dislocation core are sketched in (c) and (d), respectively. These atomic positions are superimposed to the experimental image of (a) in (e) showing good agreement, and the multislice simulation at $\Delta f = 34$ nm is presented in (f).

one 60° dislocation was located at the position of interest. Figures 4(c) and 4(d) report the model and the geometrical layout of the bonding, respectively. The atomic positions superimposed on the experimental image of Fig. 4(a) are shown in Fig. 4(e), and in Fig. 4(f) the image at 34 nm defocus calculated using the generated model is presented. As compared to the Shockley model, bonding in the perfect 60° dislocation at the GaAs/Si interface is similar. Its well-defined structure can be related to the necessary strain relaxation and therefore to the distance with the neighboring defects. In particular, we measured 5.8 nm to one Lomer and 9.4 nm to the next, giving an average value which is close to the one adequate for strain relaxation (7.31 nm). A perfect fit may not be possible due to free-surface elasticity relaxation not taken into account in the simulation (Eshelby effect[18]).

B. Interfacial 60° dislocations in interaction with neighboring ones

The 60° dislocation has been found to strongly interact with neighboring defects. In particular, the presence of a close Lomer dislocation leads to significant contrast effects which can be related to two main causes: twist effect and core dissociations.

1. Interaction with a Lomer dislocation

In the vast majority of the observed 60° dislocations, the twist effect strongly affects the image contrast. As a result, along a ⟨110⟩ zone axis the {200} and {220}, and one {111}, lattice fringe family can disappear from the image; only one {111} family dominates the contrast. This means that in the vicinity of the dislocation, the sample is no longer viewed along a [110] zone axis. It is important to notice that this takes place only inside the GaAs layer, which is less rigid than the Si substrate. In the analyzed cases, this twist is related to the Burgers vector direction of the 60° dislocation. In one case, the observed contrast could not be related to the direction of the Burgers vector; it was influenced by additional defects in the area around the dislocations as will be shown.

Typically, the contrast due to the twist effect can be seen in the area between the 60° dislocation and its Lomer closest neighbor; however, when strain is well relaxed the twist effect is minimized and images are less distorted. This is the case in Fig. 5(a), which shows the area around the 60° dislocation of Fig. 4. In spite of its perfection, one family of {111} lattice fringes is more visible near the Lomer dislocation. As indicated in the figure, the Burgers vector, identified by the start final right hand (SFRH) circuit convention and by the additional ⟨111⟩ plane, is parallel to the planes whose image is distorted by local twist. The distance between both dislocations is 6.0 nm, instead of the 7.31 nm if the local strain were to be completely relaxed.

Among the 60° dislocation analyzed, in only one of them does the contrast due to the twist not seem to be explained by the direction of the Burgers vector. As shown in Fig. 5(b), the glide plane is parallel to the {111} family which disappears from the image; however, as also can be seen, between the 60° dislocation and the Lomer one, there appears and next disappears a (111) lattice fringe, which gives a defect whose overall contribution is zero. Although it is not easy to locate the termination of the additional planes, similar behavior may be observed for (002) planes, suggesting that it is a pair of 60° dislocations with extended cores spaced by ~2.7 nm. The contribution to the local contrast of these two intermediate 60° dislocations is more important than that of the interfacial one, and this can explain the image contrast in good agreement with the other cases studied. As for the {111} plane contrast related to the screw component, the two dislocations at the left-hand side seem to add their contribution, balanced by the third 60° and the splitting of the Lomer ones.

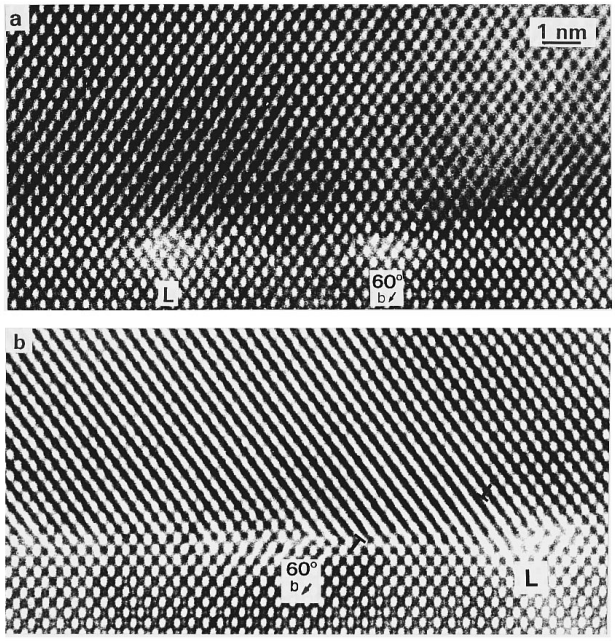

FIG. 5. Experimental images of blur-contrasted areas due to the interaction between a 60° and a Lomer dislocation: (a) slight blurring of contrast between a perfect 60° dislocation and its Lomer neighbor and (b) one case found where the (111) family parallel to the glide plane of the 60° dislocation disappears from the image.

2. Interaction with another 60° dislocation

Two of the 60° dislocations studied at the interface have been found to be adjacent, as shown in Fig. 6. In this case they have Burgers vectors contained in different {111} planes, whose resultant projection on the imaging plane co-

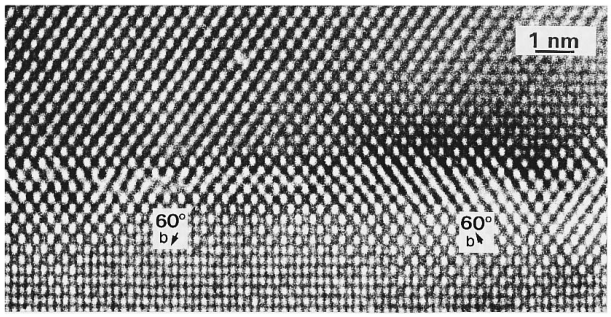

FIG. 6. Two adjacent 60° dislocations at the GaAs/Si interface. The extra (111) half-planes are not well localized.

incides with that corresponding to a Lomer dislocation ($\mathbf{b_1}+\mathbf{b_2}=1/2[1\bar{1}0]$). As the two dislocations have different glide planes, this may explain the observed clear contrast; however, they cannot be well described by the model proposed for the perfect dislocation in Sec. III B 1, since images show their terminating {111} half-planes a little more delocalized (about 1 nm). This fact can be explained by strain remaining at the interface, because the spacings between defects do not coincide with those predicted for relaxation. In particular, distance between the two 60° dislocations is 6.7 nm, and they are located at 6.9 and 4 nm from the neighboring Lomer dislocations, giving a total distance of 17.6 nm. This is therefore quite different from the ideal value of 19.49 nm (4.87 nm between the two 60° dislocations and 7.31 nm from one 60° to a Lomer one). As in the other cases, the residual strain field due to these nonideal dislocation spacings at the interface leads to dissociation of the neighboring dislocations.

C. The 60° dislocation near the interface

A rather characteristic defect, whose total Burgers vector corresponds to a typical 60° dislocation but with contrast not confined at the interface, is shown in Fig. 7(a). The extension of the anomalous contrast could be due to a dislocation line not lying parallel to ⟨110⟩ (and obviously to Eshelby twist); however, comparing the images of the whole focal series it is observed that the image does not move, suggesting that the defect runs actually along the ⟨110⟩ direction. With this in mind, the explanation of the contrast is undertaken based on the elasticity theory. As in the other cases, the Eshelby effect cannot be included in our calculations.

A close examination of the defect in question shows the presence of three {111} half-planes, implying a more complex defect. A Lomer dislocation can be detected at the interface for which additional {111} planes are split by 0.9 nm as indicated. This is an indication that the dislocation is decomposed into two partials. Moreover, on both sides of the Lomer only one family of {111} planes is visible in the GaAs layer on the micrograph. Then, in such small areas the crystal is tilted differently on each side of the Lomer dislocation. Furthermore, on the right-hand side of the Lomer, at 2 nm inside the GaAs layer, there is a 60° dislocation located in the same {111} plane as one of the partials resulting from the Lomer decomposition.

All 60° dislocations and Shockley and Frank partials might be at the origin of the extra {111} planes at the Lomer dissociation. Moreover, all of them have a screw component which can tilt the surrounding crystal area. In order to derive a definitive model describing the micrograph contrast, the anisotropic elasticity formalism was used again, and the best fit was found when the Lomer dislocation was supposed to be dissociated as follows:

$$1/2[1\bar{1}0]\rightarrow 1/6[\underset{a}{1\bar{1}2}]+1/3[\underset{b}{1\bar{1}1}].$$

Figure 7(b) represents the calculated image of the three dislocations configuration (defocus ~34 nm). Once more, the Eshelby effect does not allow to reproduce perfectly the contrast features in the cores; but the atomic positions are well

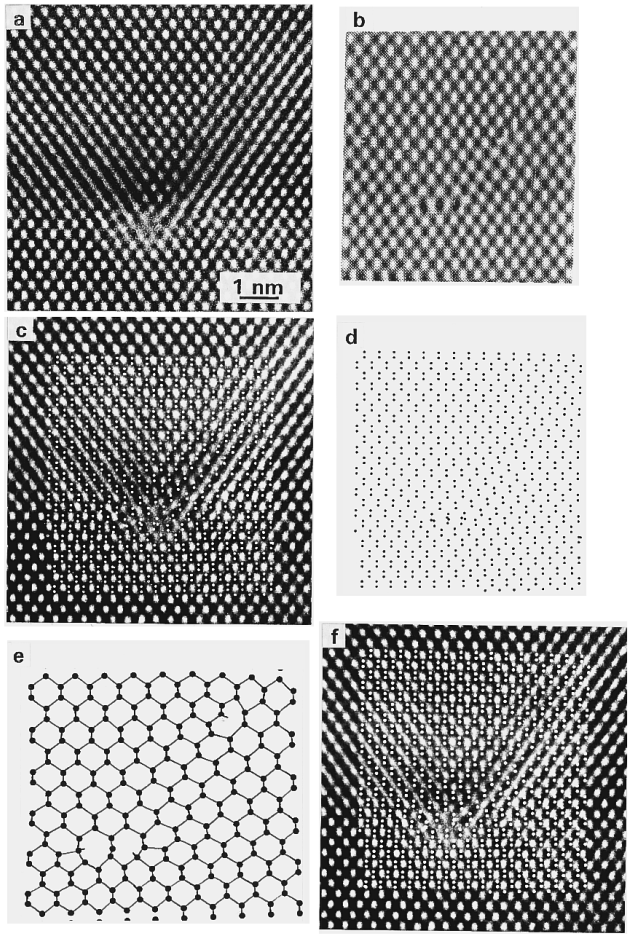

FIG. 7. An interfacial Lomer dislocation dissociated into a Shockley and a Frank partials due to the interaction with a neighboring 60° one in the GaAs layer. Experimental image in (a) and EMS elasticity multislice simulation in (b). The atomic positions used, calculated by using anisotropic elasticity, are superimposed to the experimental image in (c) and sketched in (d). However, three couples of Si and GaAs atoms appear to have very short bond lengths in the core, leading to an illogical structure. One atom of each pair has been removed from the model for simulations. The structure and bonding proposed for this case are sketched in figure (e) and in (f) the new atomic positions are superimposed onto the experimental image.

described by our model, as shown in Fig. 7(c), where the theoretical atomic positions have been superimposed to the experimental image. In Fig. 7(d) the used model is shown at the same scale. In this observation along the [110] zone axis it can be seen that the b partial is in the same {111} plane than the 60° dislocation but at the interface. The total defect made by the two partials provided by the Lomer dissociation and the 60° at 2 nm of the interface has the same Burgers vector than one lone 60° dislocation.

However, in this case the atomic positions predicted by elastical theory calculations had to be modified in order to describe the experimental images. Indeed, calculation results give atoms with very short bond lengths [Fig. 7(d)]. Since it has no physical meaning, some atoms have been suppressed in our simulations, as shown in Fig. 7(e), where a layout for bonding and structure is proposed. In Fig. 7(f) it can be seen that this new description agrees reasonably well with images obtained by experiment.

IV. CONCLUSIONS

The computed displacement field obtained by adapting the Shockley model configuration to the GaAs/Si interface has been shown to reasonably well describe the structure of the interfacial compact 60° dislocation; however, for most of the time the structure of this type of dislocations is more complex. Hence, a variety of contrast features has been observed and interpreted in terms of the directions of the Burgers vectors implied and spacings between dislocations. Interface steps have not been found to act as nucleation sites for 60° dislocations.

The 60° dislocation deformation field has been found to strongly interact with that of neighboring defects. The presence of a close Lomer dislocation leads to significant effects which can be related to the crystal twist. Moreover, interaction between two 60° dislocations seems to affect their structure itself by delocalization of the extra half-planes.

Compact cores strongly interacting with interfacial defects have also been observed for 60° dislocations out of the interface inside the GaAs layer. Anisotropic elasticity allowed us to match the experimental images with the adapted Schockley model; however, it is clear that a more complete description of the observed contrast will be attained when the Eshelby effects are taken into account.

ACKNOWLEDGMENTS

This work has been partially funded by the Spanish Interdepartmental Commission of Science and Technology, CICYT, Project MAT 93-0564. The authors would like to thank the Centro Nacional de Microelectrónica of Madrid for the growth of the samples, and the Institut Interdépartamental de Microscopie Eléctronique of the Ecole Polytechnique Fedérale of Lausanne where the observations were carried out.

[1] N. Otsuka, C. Choi, Y. Nakamura, S. Nagakura, R. Fischer, C. K. Peng, and H. Morkoç, Appl. Phys. Lett. **49**, 277 (1986).
[2] W. Shockley, Phys. Rev. **91**, 228 (1953).
[3] J. Hornstra, J. Phys. Chem. Solids **5**, 129 (1958).
[4] J. Thibault-Desseaux and J. P. Pénisson, *Dislocations*, edited by P. Veyssière, L. Kubin, and J. Castaing (CNRS, Paris, 1984).
[5] P. B. Hirsh, Mater. Sci. Technol. **1**, 666 (1985).
[6] M. Mills and P. Stadelmann, Philos. Mag. A **60**, 355 (1989).
[7] D. Gerthsen, F. A. Ponce, and G. B. Anderson, Microsc. Semicond. Mater. **100**, 23 (1989).
[8] S. I. Molina, G. Aragón, R. García, Y. González, L. González, and F. Briones, J. Electron. Mater. **22**, 567 (1993).
[9] H. L. Tsai and J. W. Lee, Appl. Phys. Lett. **51**, 130 (1987).
[10] K. I. Cho, W. K. Choo, J. Y. Lee, S. C. Park, and T. Nishinaga, J. Appl. Phys. **69**, 237 (1991).
[11] A. Vilà, A. Cornet, I. R. Morante, Y. González, L. González, and F. Briones, Mater. Lett. **11**, 155 (1991).
[12] A. Vilà, A. Cornet, J. R. Morante, and P. Ruterana, Inst. Phys. Conf. Ser. **134**, 353 (1993).
[13] A. Vilà, A. Cornet, J. R. Morante, P. Ruterana, M. Loubradou, R. Bonnet, Y. González, and L. González, Philos. Mag. A **71**, 85 (1995).
[14] F. Briones, L. González, and A. Ruiz, Appl. Phys. A **49**, 729 (1989).
[15] P. Stadelmann, Ultramicroscopy **21**, 131 (1987).
[16] R. Bonnet, G. Marcon, and A. Ati, Philos. Mag. A **51**, 429 (1985).
[17] R. Bonnet, Acta Metall. **29**, 437 (1981).
[18] J. D. Eshelby, Solid State Phys. **3**, 79 (1959).